Heritage Science

RESEARCH

Open Access

Mechanical and moisture-related properties of selected dried tempera paints

Katarzyna Poznańska[1], Aleksandra Hola[2], Roman Kozłowski[1], Marcin Strojecki[1] and Łukasz Bratasz[1*]

Abstract

Mechanical properties—modulus of elasticity and strain at break, water vapour sorption, and hygroscopic expansion of selected egg tempera and distemper paints were determined as a function of relative humidity (RH) filling in this way a critical gap in the knowledge required for the analysis of fracturing processes in paintings. The experimental work was made possible by the preparation of several tempera paints, mimicking the historical materials, in the form of large specimens. Lead white, azurite, and yellow ochre were selected as pigments, and egg yolk and rabbit skin glue as binding media. The water vapour sorption and the moisture-related swelling of the paints were dominated by the proteinaceous components of the binders. The linear hygroscopic expansion coefficient of the dried egg yolk binder was approximately 1×10^{-4} per 1% RH, several times less than the coefficient of the collagen glue (4×10^{-4} per 1% RH). The moduli of elasticity of egg tempera paints at the RH mid-range were comparable to the moduli of aged oil paints, whilst the modulus of elasticity of the distemper paint was close to values measured for animal glue-based grounds. The paints experienced the transition from brittle to ductile states on increasing RH. The egg tempera paints were found to be more brittle than the distemper paint, gessoes, and, generally, aged oil paints. The observations modify a frequently used laminar model of panel paintings in which the mismatch in the response of glue-based ground layer and wood substrate to variations in RH has been identified as the worst-case condition for the fracturing of the entire pictorial layer. This study demonstrated that tempera could be more brittle than the ground layer and in consequence more vulnerable to cracking.

Keywords Egg tempera paints, Distemper paints, Dimensional change, Water vapour sorption, Mechanical properties

Introduction

Paintings are multi-layered structures composed of a supporting substrate—mostly wood or canvas that was often sized with animal glue, a preparatory layer of ground to produce a smooth painting surface, a pictorial layer, and varnish on the top. Generally, materials constituting paintings swell or shrink when they gain or lose moisture on increasing or decreasing ambient relative humidity (RH), respectively. Hygric stresses are generated in paintings owing to different humidity-induced dimensional changes of the individual layers or the external constraint on such changes imposed by frames, stretchers, or cradles. When the stresses go beyond the critical levels cracking and flaking of the layer materials can occur.

Paintings, being the category of most valuable objects in museums, are one of the most vulnerable to temperature and RH variations. The concept that a stable climate offers structural stability to paintings has, for a long time, been derived from practical observations; a much-quoted example was the observation that the wartime storage of the collection of the National Gallery in London in a slate quarry reduced flaking previously found to occur while the collection was on exhibition in the Gallery [1]. Stabilizing RH variations became a common good practice

*Correspondence:
Łukasz Bratasz
lukasz.bratasz@ikifp.edu.pl
[1] Jerzy Haber Institute of Catalysis and Surface Chemistry, Polish Academy of Sciences, 30-239 Kraków, Poland
[2] Faculty of Conservation and Restoration of Works of Art, Jan Matejko Academy of Fine Arts in Krakow, 30-052 Kraków, Poland

which evolved into the current climate specifications for museums. Until the beginning of the 1990s, these specifications were based on the technical capabilities of climate control systems rather than an experimental or theoretical understanding of collections needs. Only then, the 'engineering' approach to the determination of allowable ranges of environmental variations was initiated by Mecklenburg's group at the Smithsonian Institution. Mechanical and moisture-related properties of materials present in painted objects—wood, canvas, glues, grounds, and oil paints—were systematically determined, including their dimensional response to climatic variations as well as the critical levels of strain at which the materials began to deform plastically or fracture [2–4]. The information was systematically enlarged and refined by other researchers [5, 6], the most recent contributions being data on the mechanical properties and dimensional change of canvases sized with animal glue and the mechanical properties of animal glues and oil paints after approximately 30 years of drying [7–9]. The use of the nanoindentation technique on submillimetre samples collected from paintings has been an attempt at obtaining mechanical parameters of original aged materials [10, 11]. Testing techniques for studying the mechanical properties of artists' paints were reviewed [12]. The analysis of moisture and mechanical response of materials and their assemblies allowed the evidence-based specifications to be developed for collections, first using simple conceptual models and then computer-aided simulations [13–15]. A comprehensive review of the existing data and evidence-based climate specifications was provided by Michalski [16]. The outcome of laboratory research and modelling has influenced relevant standards and guidelines accepted by the cultural heritage sector worldwide such as the joint declaration on environmental guidelines by the International Institute for Conservation and the International Council of Museums [17] and the chapter 'Climate Control in Museums, Galleries, Libraries and Archives' in the handbook of the American Society of Heating, Refrigeration and Air Conditioning Engineers [18]. The internationally agreed guidelines inform in turn the practice of rational climate control in many museums leading to more relaxed environmental specifications allowing the energy consumption and the use of fossil fuels to be reduced [19]. Furthermore, determining mechanical and moisture-related properties of historic materials used in paint layers allows a physical model of historical paint layers to be developed, including crack networks—the craquelure patterns that are a distinctive characteristic of the artwork, an outcome of the construction and painting techniques employed by the workshop and the artist [20]. Understanding mechanisms and processes involved in craquelure formation will allow characteristics of craquelure patterns to be coupled to a geographical area and period in which the painting was created with a long-term objective to support the authentication of paintings.

Despite the indisputable progress in the determination of properties of historic and artistic materials, the lack of data characterizing tempera paints, emphasized by the recent review of paint properties [12], strikes as a fundamental knowledge gap. Generally, 'tempera' is a binding medium that is added to pigments to obtain a paint that would adhere to a surface. Since antiquity, a large variety of natural substances such as eggs, milk, gum arabic, animal glues, wax were used as a binding medium, producing diverse tempera paints found in paintings and illuminated manuscripts, which makes it impossible to establish one universal definition of the technique [21]. In this article, the term 'egg tempera' denotes paints with egg yolk as a binder, 'distemper' paints with animal glue as a binder, and the general term 'tempera' is used for both types of paints.

Egg tempera played a particularly significant role in Italian Medieval and Early Renaissance panel paintings. Also, the richest and most frequently cited source of recipes for tempera production emerged from Italy in the early fifteenth century. In his classical work—'Il Libro dell'Arte: O, Trattato della Pittura', Cennino Cennini explained that egg tempera is a mixture of egg yolk added to pigments ground with water [22]. The icons have been painted in the Eastern Orthodox Church until today also with the use of egg tempera.

Egg yolk is composed of half water and half solids. Yolk has a highly complex heterogeneous hierarchical structure [23]. It is a lipid- and protein-rich medium. The chemical composition of egg yolk as relevant to the tempera painting technique is discussed elsewhere [24, 25]. Lipids and proteins are not separated but are associated as non-soluble particle aggregates or soluble complexes in liquid plasma. Film-forming properties largely derive from the proteinaceous components, and the lipid component functions as a plasticizer and gives flexibility to the paint. Combining NMR relaxometry and rheological measurements, a recent study demonstrated that the interaction of proteins with surfaces and edges of pigment particles is the origin of a strong change in the rheological properties of the paint [26]. Egg tempera undergoes chemical changes on thermal and light ageing, and exposure to air pollutants [27, 28]. Van den Brink [29] reported that lead-white and azurite tempera underwent different reactions during ageing—lead ions promoted hydrolysis of the ester bonds in the glycerolipids and the protein-lipid network polymer, contrary to copper ions that promoted mainly oxidation.

A distemper technique is characteristic of wall paintings on wood in China and other East Asian countries, India, and ancient Egypt. Also in European wooden architecture, the technique was used for decorating walls and architectural surfaces. According to Cennini, the recommended practice for some pigments, especially blue, was to use animal glue as a binder instead of egg yolk to avoid 'yellowing' of the paint. Animal glue is a natural polymer based on collagen. Collagen consists of long protein molecules that dissolve by heating in water, the cooled solution forms a gel, and, as the water evaporates, the gel forms a solid. Collagen gives flexibility to the distemper paint due to the ability of the molecules to stretch. Distemper is lean, which means that it contains a small amount of binder, and the paint is porous and dull.

In contrast to the extensive literature on the chemistry and photochemistry of egg tempera paints, data on their mechanical properties are scarce. Ortiz provided information on their moduli of elasticity measured at the laboratory conditions using atomic force microscopy nanoindentation while tracing changes in mechanical properties due to the ageing and biodeterioration process [30]. The obtained values ranged from 0.3 GPa for the unpigmented egg yolk to 0.7–4.25 GPa for reconstructed paints with iron oxide red, cadmium yellow, zinc white, and massicot as pigments. The nanoindentation technique was also used by Freeman et al. to determine the mechanical properties of small historic distemper samples with red ochre from the Eidsborg stave church in Norway and the obtained values of moduli of elasticity ranged from 5 to 21 GPa [11]. As demonstrated by the authors, the technique characterized the samples at the micro- and nanoscale, therefore, the determined values could be influenced by local features of the components and significantly differ from the macro-properties of bulk material. Moreover, the nanoindentation characterizes samples in the compressive mode whereas most of the macro-mechanical properties relevant for computer modelling and evaluating the risk of mechanical fracture due to an unstable environment requires to be determined in tensile tests.

Therefore, the present work has aimed to determine mechanical and moisture-related properties of selected egg tempera and distemper paints as a function of RH and fill in this way a critical gap in the knowledge required for the analysis of fracturing processes in paintings. The paper is organized as follows. The preparation of paints reconstructing as closely as possible historical paints as well as data on their composition and density are described in "Materials and methods" section, in the same section, all experimental methods used in the investigations are described. "Results and discussion" section is divided into four sub-sections that provide a systematic progression through four material properties fundamental to the assessment of risk of degradation of tempera paints: water vapour sorption, moisture-related swelling, modulus of elasticity, and strain at break. Relationships between RH and water vapour adsorption, moisture-related swelling, and moduli of elasticity are provided. The conclusions are reported at the end.

Materials and methods

The reconstructed paint layers mimicking historical paints were used in the measurements due to a lack of historical samples of large size required to determine tensile properties or moisture-related swelling. To make the composition of reconstructed paints as close as possible to the historical materials, the samples were prepared by a qualified painting restorer following the traditional recipe from Cennini's treatise.

A group of three pigments—lead white, azurite, and yellow ochre commonly used in the traditional painting practice and containing diverse metal ions were selected. As indicated in the introduction, lead-white and azurite determine different processes of chemical change in the lipid fraction of the egg yolk binder [29]. In turn, yellow ochre represents an important group of iron oxide-based pigments known to degrade the binder in oil paints. Traditional ancient lead white consisted predominantly of trilead bis(carbonate) dihydroxide ($2PbCO_3{\cdot}Pb(OH)_2$), also referred to as basic lead carbonate, that occurs naturally as the mineral hydrocerussite. The pigment was produced historically from metallic lead and vinegar, and contained lead carbonate ($PbCO_3$), corresponding to the mineral cerussite, as a minor component [31]. Therefore, in this study, both compounds were investigated—basic lead carbonate (from here hydrocerussite) from Sigma-Aldrich (SA 243582) and lead carbonate (from here cerussite) from Kremer Pigmente GmbH (KP 4600—also referred to by the producer as Cremnitz white). Azurite (KP 10200) and yellow ochre (KP 40200) were from Kremer-Pigmente GmbH.

Two types of binding medium were prepared. For egg tempera, the binding medium was prepared using fresh hen eggs. The egg yolk was separated from the egg white, and the fibrous strings were removed. Part of the fresh egg yolk was applied on a polyester foil and allowed to naturally dry for 6 months serving as reference material. The yolk was mixed with distilled water in a ratio of 1:1 w/w. The binding medium for the distemper paint was a 7% w/w water solution of rabbit skin glue (RSG). The dry RSG pearls (Kremer 63028) were soaked in cold distilled water overnight. After the glue had soaked and swollen, it was heated at around 50 °C until it was fully dissolved.

The paints were prepared by grinding the pigment with the appropriate amount of binding medium in a mortar,

adding a few more drops of water, if necessary, to make the paint easy to spread. Several pigment-to-binder ratios were tested to produce paints that met three criteria: were usable for painting, did not crack during drying, and did not chalk in a dry state. Initially, a layer of paint 200 µm thick was applied on a polyester film, and after drying it was detached from the substrate. The obtained paint films were too brittle and therefore not suitable for the tensile tests. To overcome this limitation, the paints were cast into a mould and left to dry at ambient conditions (23–25 °C, 50% RH) for 6 months. Large blocks of dried cast materials around 15 mm thick (Fig. 1) were machined into small specimens 6 mm × 6 mm × 80 mm.

Two aspects need to be considered for large specimens of paints tested in this study when compared to paint films: smaller surface-to-volume ratio and more likely presence of air bubbles and voids as structural flaws. Moduli of elasticity measured for large specimens may be underestimated because the actual cross-section of the specimen is smaller than the one calculated from the specimen's size. For the same reason, moisture-related swelling measured for large specimens may be also underestimated. On the other hand, values of the strain at break may be smaller for paint films due to the effect of near-surface structural flaws at which cracking is initiated on the specimen loading.

Details of the prepared paints are given in Table 1. The ratio of the pigment to the binder in dried paints is expressed in % as the pigment volume concentration (PVC): $PVC = P/(P+B)\cdot 100$, where P is the volume of the pigment and B is the volume of the dried binder. It was assumed in the calculations that all water added during preparation and contained in the egg yolk evaporated when the paint dried. The volume of an ingredient was calculated from mass divided by the material density. Pigments were stored at approximately 23–25 °C, 40–50% RH before weighing. The densities of the fresh egg yolk and RSG were 1.03 [32] and 1.1 kg/dm^3, respectively, and of the pigments—according to manufacturers' information—hydrocerussite 7.1, cerussite 6.4, azurite 4.0, yellow ochre 3.5 kg/dm^3. The calculations assumed that water constituted half of the mass of the fresh yolk. Bulk density was determined from the

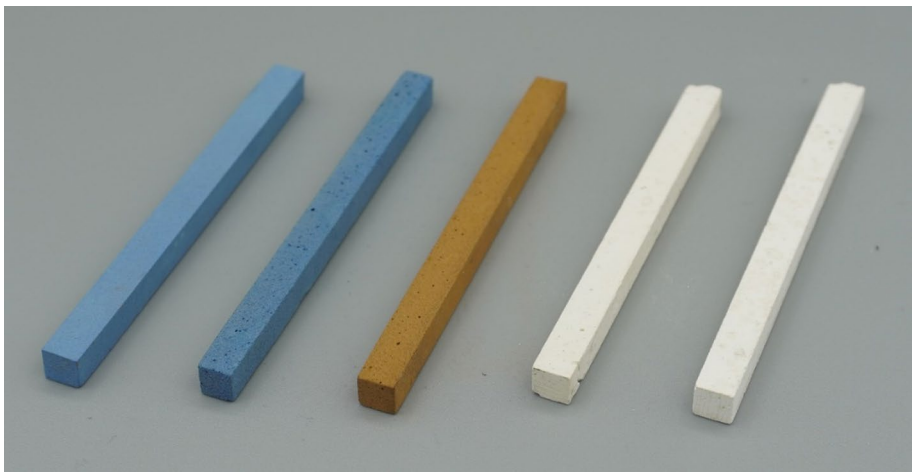

Fig. 1 Specimens of a distemper paint with azurite and egg tempera paints with azurite, yellow ochre, cerussite, and hydrocerussite as pigments (from left to right)

Table 1 Composition, bulk density, and porosity of tempera paints investigated in the study

Pigment	Binder	Ratio of pigment to binding medium in wet paint (w/w)	Pigment content in wet paint (% w/w)	Pigment content in dry paint (% w/w)	Pigment content in wet paint (% v/v)	PVC in dry paint (% v/v)	Bulk density (kg/dm^3)	Porosity (%)
Cerussite	Egg yolk	2.20	69	90	26	63	2.27	47
Hydrocerussite	Egg yolk	2.94	75	92	30	66	2.83	53
Yellow ochre	Egg yolk	2.14	68	90	39	75	1.66	53
Azurite	Egg yolk	2.95	75	92	44	78	2.05	57
Azurite	RSG	2.29	70	97	37	90	2.14	58

average mass and dimensions of 5 samples of each type of paint stored at approximately 23–25 °C, 40–50% RH.

Porosity of dried paints was calculated from their bulk density and PVC to be around 50% (Table 1). However, the porosity structure differed between the paints. As one can observe in Fig. 1, whilst the distemper paint shows a uniform structure of small pores, the specimens of egg tempera paints contain large air bubbles and voids in their structure.

Water vapour sorption isotherms were measured for single specimens of pigments, unpigmented dried yolk, and paints with the use of a vacuum microbalance from CI Electronics in the full RH range (5 to 90%) at 25 °C. A sample of around 0.1 g was weighed and outgassed prior to a measurement under a vacuum of a residual pressure of less than 10 Pa. The vacuum was maintained until a constant mass was obtained, then subsequent portions of water vapour were introduced. The moisture content in a sample exposed to a given RH eventually attained a constant level termed the equilibrium moisture content (EMC). EMC is expressed as the increase of the initial mass of the outgassed sample in percent. Samples were considered to have reached EMC when the mass changes after 30 min were less than 5 μg in 3 min. The measurements were repeated three or four times, and an average isotherm was calculated except of the dried egg yolk. For this material, water vapour sorption process was slow, especially at high RH. The reason was probably the transition from a dry solid to a gel with increasing RH. Therefore, the isotherm recorded for the maximum time of equilibration of 2 weeks justified experimentally is published in this study. To each adsorption and desorption point an exponential growth curve was fitted to find the true EMC value. The relative uncertainty of the sorption measurements was approximately 10% except for dried egg yolk at a high RH level of 90%.

Swelling isotherms were determined in a Universal Testing Machine Inspekt Table 10 kN (UTM) from Hegewald & Peschke MPT GMBH (Nossen, Germany) typically using specimens 50 mm long. The specimen was mounted in the upper jaw and the lower part was free to move in the vertical direction. Three pairs of reference points were applied with a marker evenly across the specimen width. The elongation was measured by optical extensometer One from the same manufacturer as UTM with an accuracy of 2 μm at a constant temperature of 25 °C as a function of RH, starting at 30% and finishing at 90% with an increment of 10%. Each new RH level was maintained until a constant length of sample was obtained. The time of specimen equilibration was approximately 6 h at RH levels between 30 and 70%, 10 h at 80%, and 24 h at 90% RH. The strain was calculated as an average of three length measurements for three pairs of reference points. The uncertainty of the measurement is estimated as 10% of the value.

Tensile properties were determined using UTM equipped with a 100 or 500 N load cell depending on the specimen strength. The specimen was glued into flexible Cardan joints, using a high-stiffness epoxy resin, to ensure a linear alignment and prevent cracking due to bending during the load application. The effective length of the glued specimens was approximately 60 mm. Each specimen investigated was preconditioned at a given RH level in a climatic chamber for 1 day. UTM was equipped with a sealed compartment connected to the climatic chamber, which allowed RH to be precisely controlled at four RH levels: 30, 50, 75, and 90%, and the temperature at 25 °C. The displacement was measured using a mechanical extensometer from the same manufacturer as UTM with a gauge length of 50 mm and an accuracy of 0.2 μm or in some cases with the optical extensometer which, however, was less accurate—2 μm as indicated above. The rate of elongation was 0.125 mm/min corresponding to a strain rate of 0.0042%/s. The specimen with the mechanical extensometer attached to one side was preloaded to a level for which the elongation was fully reversible and then unloaded. Such a procedure ensured better alignment of the specimen and the Cardan joints. The preloading level was 10 N, 5 N, and 2 N for RH 30% and 50%, 75%, and 90%, respectively. The cycle was repeated and, after unloading, the position of the mechanical extensometer was changed to the opposite side of the specimen. Finally, the load was increased in the displacement-controlled mode until the failure of the specimen. The load-extension data obtained for both positions of the extensometer were used to calculate the average load-extension curve. The lead white specimens at the highest RH level were very ductile and the attachment of the mechanical extensometer was causing bending of the specimen. Therefore, the optical extensometer was used to measure elongation instead. The modulus of elasticity was determined from the slope of the load-extension curve in the linear region not exceeding 0.02%. Values of the modulus and strain at break for each paint were determined as the mean values from between two and four loading experiments at each RH level.

Results and discussion

Water vapour sorption

The relationship between EMC and RH for dried egg yolk is shown in Fig. 2. Its characteristic feature is a hysteresis loop, that is to say, higher moisture content during desorption when compared to that during adsorption, extending to low RH values. The phenomenon is associated with the swelling of a non-rigid binder structure in the course of adsorption so that the effect is in fact a

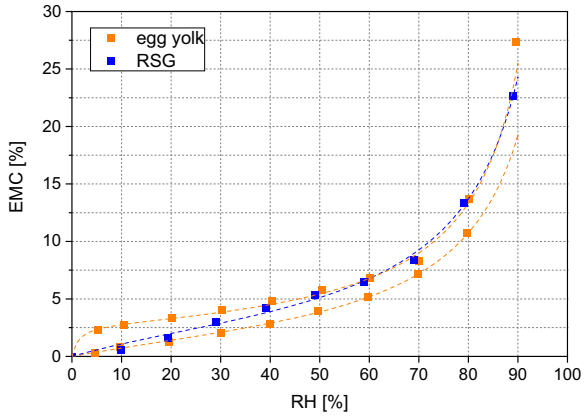

Fig. 2 Equilibrium moisture content versus RH for binders (the adsorption data for RSG taken from ref. [14]). The experimental data are compared with the curves calculated from the least-square regression of the data to the GAB equation

manifestation of elastic hysteresis [33]. The water vapour adsorption data for RSG taken from Fig. 2 in ref. [14]. are shown for comparison.

The Guggenheim–Anderson-de Boer (GAB) three-parameter equation was used to describe the sorption of water vapour on the investigated materials. The equation is widely employed to describe the full shape of the type II isotherm in the IUPAC 1985 classification [33]. Such isotherm type indicates the monolayer-multilayer physisorption in which an adsorbed surface layer progressively thickens as the vapour pressure is increased up to saturation pressure. The GAB equation was fitted to experimental points in the range from 0 to 80% RH which covers RH conditions relevant to the preservation of paintings indoors:

$$EMC(RH) = \frac{V_m \cdot c \cdot k \cdot RH/100}{(1 - k \cdot RH/100) \cdot (1 + (c-1) \cdot k \cdot RH/100)}$$

where EMC is the equilibrium moisture content in percent, RH—relative humidity in percent, V_m—the monolayer capacity in the same units as EMC, c—an energy constant related to the difference of free enthalpy (standard chemical potential) of water molecules in the upper sorption layers and in the monolayer, and k—the third parameter, related in turn to the difference of free enthalpy of water molecules in the pure liquid and the upper sorption layers.

Curves calculated using the GAB equation are compared in Fig. 2 with the experimental data. For the dried yolk, the GAB constants were determined separately for the adsorption and desorption branches. The GAB constants, their uncertainties, and the coefficient of determination R^2 are given in Table 2 for all materials investigated. Owing to the hysteresis loop, only the adsorption branch yields meaningful physical parameters—the monolayer capacity and the energy constant.

Table 2 GAB constants obtained from the fit of water vapour sorption isotherms to the experimental data

	V_m	c	k	R^2
Pigments				
Yellow ochre	0.70 (0.04)	16.2 (3.4)	0.81 (0.03)	0.978
Azurite	0.152 (0.01)	15.2 (3.8)	0.81 (0.03)	0.97
Hydrocerussite	0.028 (0.009)	8.3 (5)	0.67 (0.17)	0.89
Cerussite	0.024 (0.001)	5.1 (1.9)	1 (fixed)	0.96
Binder				
Rabbit skin glue adsorption	3.44 (0.06)	3.7 (1.6)	0.96 (0.04)	0.99
Egg yolk				
Adsorption	2.75 (0.13)	2.95 (0.3)	0.96 (0.01)	0.99
Desorption	2.78 (0.13)	75 (55)	0.99 (0.02)	0.99
Egg tempera				
Yellow ochre	0.74 (0.08)	13.6 (4.1)	0.73 (0.06)	0.94
Azurite	0.25 (0.03)	17.3 (5.2)	0.71 (0.06)	0.95
Hydrocerussite	0.21 (0.01)	7.4 (0.6)	0.85 (0.01)	1.00
Cerussite	0.25 (0.01)	12.1 (0.7)	0.81 (0.01)	1.00
Distemper				
Azurite	0.25 (0.02)	17.9 (5.2)	0.88 (0.03)	0.97

The EMC-RH plots for pigments are shown in Fig. 3. The pigment sorption did not exhibit any significant hysteresis loops.

The egg yolk and RSG sorb significantly more water than pure lead white pigments and azurite. Relatively high sorption by yellow ochre, almost 3% at 90% RH, is caused by the 20% weight content of clay minerals, predominantly kaolinite, in the pigment as determined by x-ray powder diffraction in this study (data not shown). The measurements

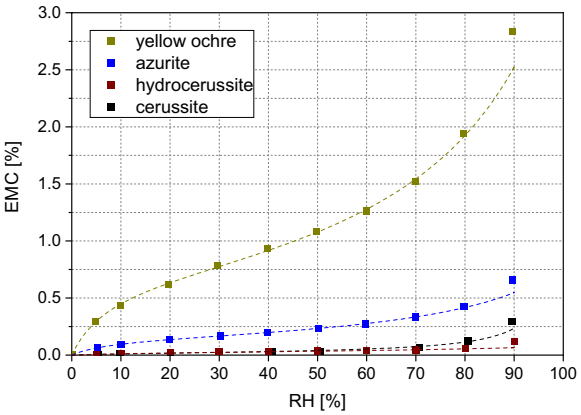

Fig. 3 Equilibrium moisture content versus RH for pigments. The experimental data are compared with the curves calculated from the least-square regression of the data to the GAB equation

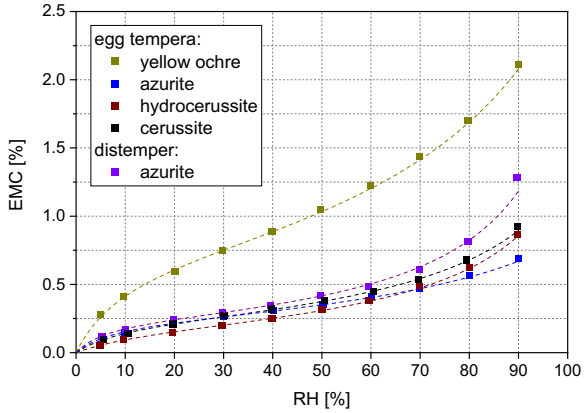

Fig. 4 Equilibrium moisture content versus RH for the tempera paints investigated. The experimental data are compared with the curves calculated from the least-square regression of the data to the GAB equation

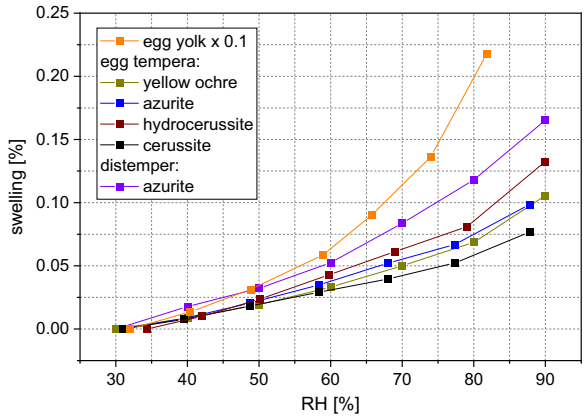

Fig. 5 Moisture-related strain for the tempera paints investigated

agree well with water sorption data for two yellow ochre pigments reported in [34].

The water vapour sorption by the paints was approximately a sum of the sorption by the binder and the pigment when the pigment-to-binder ratio was taken into account (Fig. 4). As a result, the sorption by the paints with hydrocerussite, cerussite, and azurite was very similar independently of the binder used. In turn, the paints containing yellow ochre sorbed more than twice as much as other paints, particularly in the lower RH range.

Moisture-related swelling

The direct effect of moisture sorption by paints is their swelling. Moisture-related swelling of the paints investigated in the RH range of 30–90% is shown in Fig. 5.

The moisture-related swelling of paints depends on swelling characteristics of pigment particles and binder, their respective contents in the dried paint—reflected in the pigment volume concentration PVC, and the microscopical geometry of particles and binder. As the volume concentration of pigments, which adsorb little moisture, is high in paints (60–90%, see Table 1), the overall swelling of paints is an order of magnitude smaller than that of the binders. The microstructure of the pigment-binder system can further reduce the swelling of paints. The linear hygroscopic expansion coefficient $\alpha_{RH,binder}$ for the dried egg yolk and $\alpha_{RH,paint}$ for the paints were obtained by the linear regression of the data in low and high RH ranges of 30–40% and 70–90%, respectively (Table 3). The hygroscopic expansion coefficient for the binders ($\alpha_{RH,binder}$) was calculated for the low RH range using the formula derived by Michalski [35]:

$$\alpha_{RH,binder} = \alpha_{RH,paint}\left(1 + \frac{1}{\left(\frac{100}{PVC}\right)^{1/3} - 1}\right)$$

Table 3 The linear hygroscopic expansion coefficient of paints and dried yolk measured in the study and calculated for their components

RH range	30–40%			70–90%
Linear hygroscopic expansion coefficient	$\alpha_{RH,paint}$ [10^{-5} per 1% RH]	$\alpha_{RH,binder}$ [10^{-4} per 1% RH]	$\alpha_{RH,protein}$ [10^{-4} per 1% RH]	$\alpha_{RH,\ paint\ /binder}$ [10^{-5} per 1% RH]
Dried egg yolk		1.6 (measured)	4.9	79
Egg tempera				
Yellow ochre	1.0 (0.85[a])	0.9	2.8	2.8
Azurite	1.0	1.3	3.9	2.4
Hydrocerussite	1.3	1.0	3.1	3.4
Cerussite	1.0	0.7	2.2	1.9
Distemper				
Azurite	1.6	4.6	4.6	4.1

[a] Value reflecting the moisture-related swelling of the binder only

In Michalski's model, particles of an assumed spherical shape are embedded in the binder and well separated one from another at the start of drying. The binder dries as a semirigid gel, and the binder molecules are assumed to maintain their relative position during the process. Since most of the binder can be assigned to separate spherical shells around pigment particles, the drying is envisaged as shrinkage of these shells. The model allows the interparticle separation in dry paint to be calculated—its relative change on swelling of the disks of binder between pigment particles is equivalent to the hygroscopic expansion coefficient of a paint from which, in turn, the coefficient for binder can be calculated for the given paint composition reflected in the PVC value.

As lead white pigments and azurite adsorb very little moisture, it was assumed that the moisture-related swelling of the paints containing the pigments is solely due to the swelling of the binders. In contrast, clay in natural earth pigments like yellow ochre significantly contributes to the swelling of paints containing them with increasing RH. Mecklenburg determined the moisture-related swelling isotherm for a dried yellow ochre oil paint which is dominated by the response of the pigment given the negligible response of the aged oil binder ([3], Fig. 31). It can be assessed from this swelling isotherm that the hygroscopic expansion coefficient of the pigment is 1.5×10^{-6} per 1% RH in the RH range of 30–40%. After the value was subtracted from the coefficient calculated for the yellow ochre tempera paint, the contribution of the binder to the coefficient was 8.5×10^{-6} per 1% RH and such value was used to calculate $\alpha_{RH,binder}$ for this particular paint. Finally, it was assumed that the swelling of egg tempera paints is only due to the swelling of the proteinaceous component of the binder which constitutes just one-third of the yolk solid phase (Table 2 in ref. [25]). . The hygroscopic expansion coefficient of proteins in each binder $\alpha_{RH,proteins}$ was then calculated, the binder in the distemper paint was assumed to be pure collagen.

The coefficient for the glue binder in the distemper paint agrees with values of 4×10^{-4} per 1% RH and 4.2×10^{-4} per 1% RH provided by Mecklenburg [36] and Rachwał et al. [14], respectively, and is similar to the coefficient for the egg yolk protein measured. The coefficient for yolk proteins calculated from the swelling data for egg tempera with the same pigment—azurite—was somewhat lower, and further decreased to approximately 3×10^{-4} per 1% RH for hydrocerussite and yellow ochre, indicating the effect of pigment's morphological characteristics on the dimensional response of the binder in the paint. The effect is particularly evident for the paint with cerussite. SEM micrographs shown in Fig. 6 reveal a difference in the crystal morphology of cerussite and hydrocerussite. While hydrocerussite is a coarse-crystalline material with single crystals generally well separated from each other, cerussite consists of agglomerations of small pigment particles into large clumps. The effective dimensional response of the binder surrounding the agglomerates is reduced as indicated by a much lower value of the coefficient for the egg yolk protein in the tempera paint with hydrocerussite.

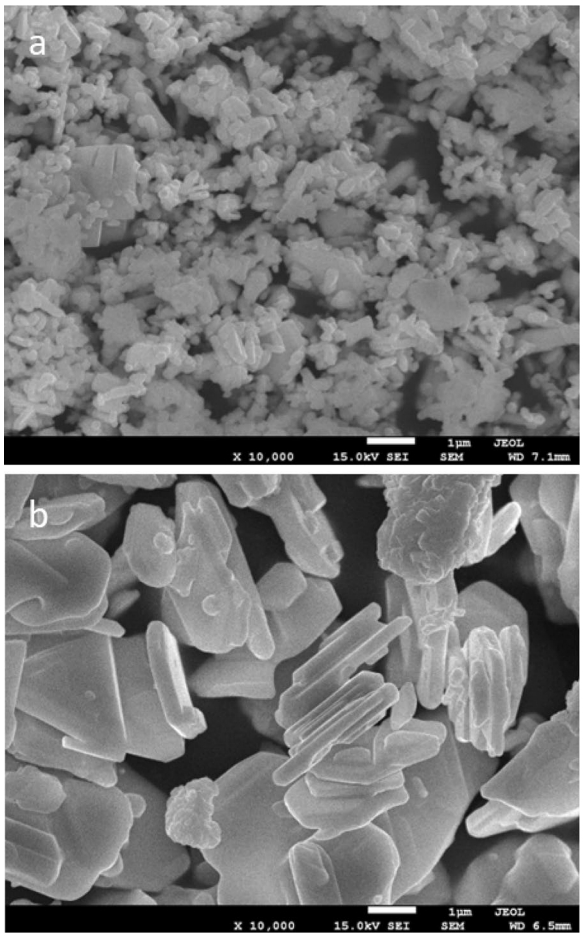

Fig. 6 SEM micrographs: **a** cerussite, **b** hydrocerussite

Modulus of elasticity

An example of single measurements of stress-strain curves for egg tempera paints with cerussite as a pigment obtained at various RH levels is presented in Fig. 7. Strain is expressed as a change in the specimen's original length in percent. The evolution of plots with RH is representative of all paints investigated.

The increase in tensile strength and stiffness observed for the paint with decreasing RH is accompanied by a reduction in the strain at break. The initial moduli of elasticity, determined from the slope of the stress-strain curve at low strains not exceeding 0.02% for egg tempera and distemper paints with various pigments,

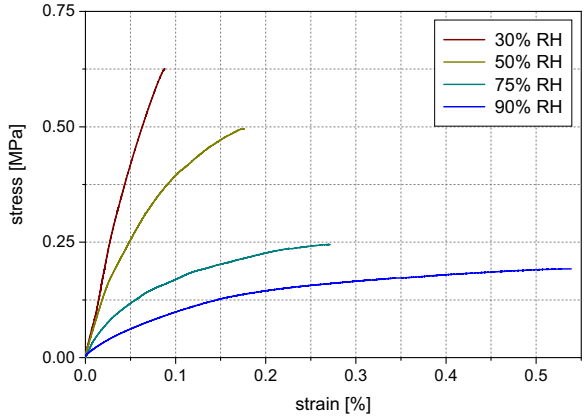

Fig. 7 Stress-strain curves for egg tempera paint with cerussite obtained at varying RH levels

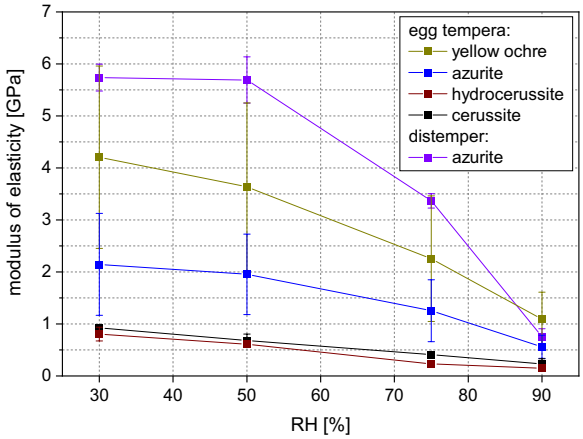

Fig. 8 Moduli of elasticity for various tempera paints and RH levels. Error bars indicate one standard deviation

are summarized in Fig. 8. The moduli of elasticity for egg tempera paints are comparable to the moduli of oil paints, dried for relatively long periods exceeding 20 years [9]. As the mechanical properties of paints significantly depend on pigments present in their composition, a direct comparison is possible only for the paints with lead white—the values of moduli of elasticity at approximately 50% RH were 0.7 and 1 GPa for egg tempera with hydrocerussite or cerussite (this study), or oil paint aged for 30 years [9], respectively. In contrast to paints with lead white, a dramatic difference is observed between the moduli of elasticity of egg tempera and oil paints containing pigments with iron oxides-hydroxides like yellow ochre. Whilst the egg tempera paint with yellow ochre investigated in this study formed a stiff film with the modulus of elasticity of 3.5 GPa at approximately 50% RH, paints with the same pigment and oil as the binder experience a serious loss of stiffness combined with increasing plasticity as curing time goes on, owing to early hydrolysis reactions in the binder taking place [3, 37]. As the tempera paints are water-based, the drying process predominantly involves evaporation of the solvent with proteins creating a polymerized network that gives stiffness to the paint.

The modulus of elasticity of the distemper paint is close to values measured for animal glue-based ground (gesso) [14, 38]. The paints experience a decrease in the modulus of elasticity with increasing RH (Fig. 8). The loss of stiffness is particularly pronounced for RH higher than 75%, independently of the type of tempera or the pigment. The observation points to a transition from a brittle to ductile (gel-like) state. The proteinaceous binder in egg tempera was found to mirror such transition in the glue-based grounds [38] and oil paints [34].

Strain at break

The strain at break determined for the paints investigated is shown in Fig. 9. As expected, the distemper paint has strain at break similar to that of gesso up to 65% RH as structurally the materials are identical except for different pigments which are inert solids. The strain at break of egg tempera paints is below 0.1% at an RH level of 30% and gradually increases with RH to between 0.2 and 0.5% at 90%. The materials are more brittle at the RH mid-range than gesso with the strain at break of approximately 0.2%. Furthermore, the values measured at 50% RH are generally lower than those determined for oil paints even dried for long periods ([9], Fig. 6). For the paints with lead white pigments for which a direct comparison of the mechanical properties is possible that difference is striking 0.15% and 1% for egg tempera or oil paint aged for

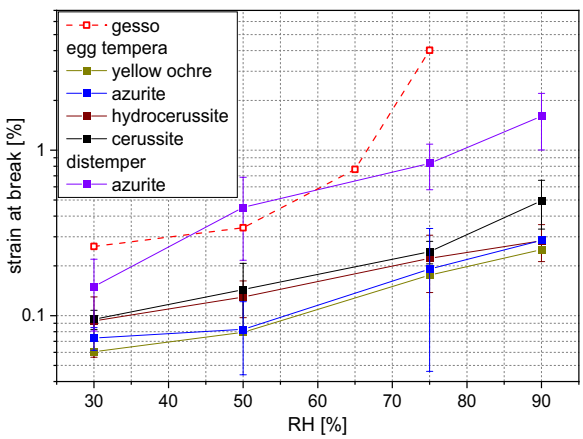

Fig. 9 Strain at break for various tempera paints at various RH levels. The red dashed line indicates strain at break typically measured for gesso (data from Fig. 4 in ref. [14]).

30 years, respectively. The tensile strength of the paints investigated is shown in Fig. 10.

The values of strain break determined in this study for egg tempera paints further support the necessary modification of a frequently used laminar model of paintings subjected to variations of RH proposed recently [9]. The model is based on the principle of superposition and assumes that the structural response of a painting is obtained by superimposing individual responses of its components: wood or canvas support, animal glue size, a preparatory ground layer, paint, and varnish. So far, the gesso has been considered the component of the pictorial layer that has the lowest strain break and cracks first when the layer experiences an increase in the tensile strain. This study demonstrates that tempera paints, similarly to some oil paints, are more brittle than gesso and may crack first under tensile strain.

Conclusions

Panel paintings are in a category of heritage objects most vulnerable to temperature and RH variations and their climate-induced damage is an important type of risk in most museum collections and historical interiors. Developing evidence-based environmental specifications for the cultural heritage sector requires collecting data on mechanical and moisture-related properties of historic materials that can supply input into algorithms modeling risk of climate-induced damage of materials and their assemblies and provide a frame of reference for conservation and museum professionals. Furthermore, properties of historic materials used in paint layers allow understanding of mechanisms of crack pattern formation—the craquelures—which are a distinctive characteristic of the artwork. Since the 1990s, such properties of materials present in painted objects—wood, canvas, glues, grounds, and oil paints—were systematically determined, as analysed in detail in the introduction. The lack of data characterizing tempera paints has remained so far a fundamental knowledge gap.

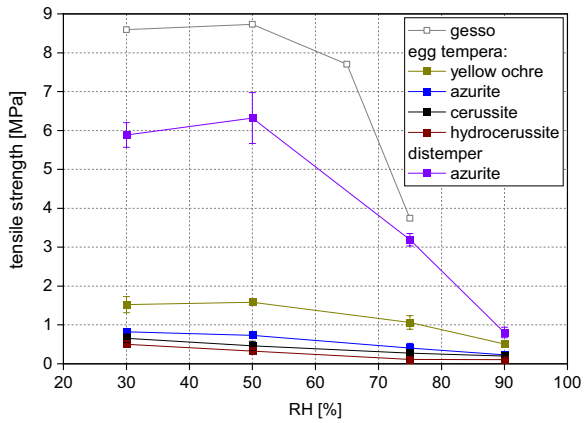

Fig. 10 Tensile strength for various tempera paints at various RH levels. The relationship for gesso was taken from ref. [14].

In this study, the preparation of several tempera paints, mimicking the historical materials, in the form of large specimens enabled laboratory measurements of their moisture-related and mechanical properties. The water vapour sorption by the paints was approximately a sum of the sorption by the binder and the pigment if the pigment-to-binder ratio was taken into account. The egg yolk and glue binders were found to sorb significantly more water than lead white pigments and azurite, only yellow ochre visibly contributed to the water sorption of the paint owing to the presence of kaolinite in the pigment. The direct effect of moisture sorption by paints is their swelling. The linear hygroscopic expansion coefficient of the egg yolk binder was determined to be approximately 1×10^{-4} per 1% RH, several times less than the coefficient of the collagen glue (4×10^{-4} per 1% RH). The moduli of elasticity for egg tempera paints were comparable to the moduli of aged oil paints, whilst the modulus of elasticity of the distemper paint was close to values measured for glue-based grounds. The paints experienced a decrease in the modulus of elasticity with increasing RH, mirroring the transition from the brittle to ductile state documented in earlier research for glue-based grounds and oil paints.

The egg tempera paints were found to be more brittle at the RH mid-range than the distemper paint, gessoes, and, generally, aged oil paints. The observations further support the necessary modification of the frequently used laminar model of panel paintings in which the mismatch in the response of gesso and unrestrained wood substrate in the direction across the grain to variations in RH has been identified as the worst-case condition for the fracturing of the entire pictorial layer. This study demonstrated that tempera paints investigated, similarly to some oil paints, are more brittle than gesso and in consequence can crack first when the pictorial layer experiences an increase in tensile strain.

It is believed that the mechanical and moisture-related properties of the tempera paints determined in this study are close to those of historical paints. The glue and egg yolk binders predominantly solidify and harden through gradual loss of water through evaporation. The glue binder contains only proteins and no significant aging effect on the physical properties of the dried material is expected. In turn, though the egg yolk contains both proteins and lipids, it is a polymer network of proteins formed during water evaporation that primarily determines the properties of the dried paint film, with a lesser contribution of the small lipid part whose molecular

composition is known to evolve owing to chemical reactions with oxygen. Indeed, the high stiffness of the egg tempera paint with yellow ochre established in this study points to an effective hardening mechanism not weakened by hydrolysis of the lipid component well-established for oil paints containing iron oxides-hydroxides.

Abbreviations

GAB	Guggenheim–Anderson-de Boer
PVC	Pigment volume concentration
RH	Relative humidity
RSG	Rabbit skin glue
SEM	Scanning electron microscopy
UTM	Universal testing machine
v/v	Volume per volume
w/w	Weight per weight

Acknowledgements
The authors are grateful to Sonia Bujok, Arkadiusz Janas, and Wiktor Kotlarz for their help and advice during the measurements. The authors thank Daria Napruszewska and Dorota Duraczyńska for the x-ray powder diffraction and scanning electron microscopy measurements, respectively.

Author contributions
ŁB and KP planned research methods and experiments, AH and KP prepared the specimens, KP and MS carried out the measurements, KP, RK, ŁB analysed and interpreted results, RK wrote the first draft of the manuscript. All authors developed and approved the final manuscript.

Funding
The research leading to these results has received funding from the Norwegian Financial Mechanism 2014–2021, project registration number 2019/34/H/HS2/00581, and the statutory research fund of the Jerzy Haber Institute of Catalysis and Surface Chemistry Polish Academy of Sciences.

Availability of data and materials
All data needed to evaluate the conclusions in the paper are presented in the paper. Additional data related to this paper may be requested from the corresponding author.

Declarations

Competing interests
The authors declare no competing interests.

Received: 11 October 2023 Accepted: 14 January 2024
Published online: 25 January 2024

References

1. Davies M, Rawlins I. The war-time storage in Wales of pictures from the National Gallery, London. Trans Hon Soc Cymmrodorion. 1945;179–93.
2. Mecklenburg MF, Tumosa CS, Erhardt D. Structural response of painted wood surfaces to changes in ambient relative humidity. In: Dorge V, Howlett FC, editors. Painted wood: history and conservation. Los Angeles: The Getty Conservation Institute; 1998. p. 464–83.
3. Mecklenburg MF. Determining the acceptable ranges of RH and T in museums and galleries, part 1. A report of the Museum Conservation Institute, the Smithsonian Institution; 2011. http://www.si.edu/mci/english/learn_more/publications/reports.html. Accessed 28 Jan 2023.
4. Mecklenburg MF, Tumosa CS, Erhardt D. New environmental guidelines at the Smithsonian Institution. Papyrus (Int Assoc Mus Facil Adm). 2004;5(3):16–7.
5. Hagan EWS. Thermo-mechanical properties of white oil and acrylic artist paints. Prog Org Coat. 2017;104(3365):28–33.
6. Luimes RA, Suiker ASJ, Verhoosel CV, Jorissen AJM, Schellen HL. Fracture behaviour of historic and new oak wood. Wood Sci Technol. 2018;52(5):1243–69.
7. Janas A, Fuster-López L, Krarup Andersen C, Escuder AV, Kozłowski R, Poznańska K, Gajda A, Scharff M, Bratasz Ł. Mechanical properties and moisture-related dimensional change of canvas paintings—canvas and glue sizing. Herit Sci. 2022;10:160.
8. Bridarolli A, Freeman AA, Fujisawa N, Łukomski L. Mechanical properties of mammalian and fish glues over range of temperature and humidity. J Cult Herit. 2022;53:226–35.
9. Janas A, Mecklenburg MF, Fuster-López L, Kozłowski R, Kékicheff P, Favier D, Krarup Andersen C, Scharff M, Bratasz Ł. Shrinkage and mechanical properties of drying oil paints. Herit Sci. 2022;10:181.
10. Łukomski M, Bridarolli A, Fujisawa N. Nanoindentation of historic and artists' paints. Appl Sci. 2022;12: 1018.
11. Freeman AA, Fujisawa N, Bridarolli A, Bertolin C, Łukomski M. Microscale physical and mechanical analyses of distemper paint: a case study of Eidsborg stave church, Norway. Stud Conserv. 2023;68(1):54–67.
12. DePolo G, Walton M, Keune K, Shull KR. After the paint has dried: a review of testing techniques for studying the mechanical properties of artists' paint. Herit Sci. 2021;9:68.
13. de Willigen P. A mathematical study on craquelure and other mechanical damage in paintings. Delft: Delft University Press; 1999.
14. Rachwał B, Bratasz Ł, Krzemień L, Łukomski M, Kozłowski R. Fatigue damage of the gesso layer in panel paintings subjected to changing climate conditions. Strain. 2012;48(6):474–81.
15. Bosco E, Suiker ASJ, Fleck NA. Moisture-induced cracking in a flexural bilayer with application to historical paintings. Theor Appl Fract Mech. 2021;112: 102779.
16. Michalski S. Climate guidelines for heritage collections: where we are in 2014 and how we got here. In: Stauderman S, Tompkins WG, editors. Proceedings of the Smithsonian Institution summit on museum preservation environment. Washington, DC: Smithsonian Institution Scholarly Press; 2016. p. 7–32.
17. Bickersteth J. IIC and ICOM-CC 2014 declaration on environmental guidelines. Stud Conserv. 2016;61:12–7.
18. Chap. 24: Museums, galleries, archives and libraries. In: ASHRAE handbook. Peachtree Corners. American Society of Heating and Air-Conditioning Engineers; 2019.
19. Kramer RP, Schellen HL, van Schijndel AWM. Impact of ASHRAE's museum climate classes on energy consumption and indoor climate fluctuations: full-scale measurements in museum Hermitage Amsterdam. Energy Build. 2016;130:286–94.
20. Jamalabadi MYA, Zabari N, Bratasz Ł. Three-dimensional numerical and experimental study of fracture saturation in panel paintings. Wood Sci Technol. 2021;55:1555–76.
21. Reinkowski-Häfner E. Tempera: narratives on a technical term in art and conservation. In: Dietemann P, Neugebauer W, Ortner E, Poggendorf R, Reinkowski-Häfner E, Stege H, editors. Tempera painting 1800–1950. Experiment and innovation from the nazarene movement to abstract art. London: Archetype Publications Ltd; 2019. p. 21–32.
22. d'Andrea CC. The Craftman's handbook (Il Libro dell'Arte). Translated by Thomson Jr DV. New York: Dover Publications; 1954.
23. Anton M. Egg yolk: structures, functionalities and processes. J Sci Food Agric. 2013;93(12):2871–80.
24. Boon JJ, Peulvé S, van den Brink OF, Duursma MC, Rainford D. Molecular aspects of mobile and stationary phases in ageing tempera and oil paint films. In: Bakkenist T, Hoppenbrouwers R, Dubois H, editors. Early Italian paintings: techniques and analysis. symposium, Maastricht, 9–10 October 1996. Limburg Conservation Institute; 1997. p. 35–56.
25. Phenix A. The composition and chemistry of eggs and egg tempera. In: Bakkenist T, Hoppenbrouwers R, Dubois H, editors. Early Italian paintings: techniques and analysis, symposium, Maastricht, 9–10 October 1996. Limburg Conservation Institute; 1997. p. 11–20.
26. Fanost A, de Viguerie L, Ducouret G, Mériguet G, Walter P, Glanville L, Rollet ALL, Jaber M. Connecting rheological properties and molecular dynamics of egg-tempera paints based on egg yolk. Angew Chem Int Ed. 2022;61: e202112108.
27. Arbizzani R, Casellato U, Fiorin E, Nodari L, Russo U, Vigato PA. Decay markers for the preventative conservation and maintenance of paintings. J Cult Herit. 2004;5(2):167–82.

28. Meilunas RJ, Bentsen JG, Steinberg A. Analysis of aged paint binders by FTIR spectroscopy. Stud Conserv. 1990;35(1):33–51.
29. van den Brink OF, Eijkel GB, Boon JJ. Dosimetry of paintings: determination of the degree of chemical change in museum-exposed test paintings by mass spectrometry. Thermochim Acta. 2000;365(1–2):1–23.
30. Ortiz Miranda AS. Development of analytical methods for the characterization of tempera paintings at micro and nanoscale and their deterioration and biodeterioration process. Thesis, Universitat Politècnica de València; 2017.
31. Gettens RJ, Kühn H, Chase WT. 3. Lead white. Stud Conserv. 1967;12(4):125–39.
32. Kumbár V, Strnková J, Nedomová Š, Buchar J. Fluid dynamics of liquid egg products. J Biol Phys. 2015;41:303–11.
33. Sing KSW, Everett DH, Haul RAW, Moscou L, Pierotti RA, Rouquerol J, Siemieniewska T. Reporting physisorption data for gas solid systems with special reference to the determination of surface area and porosity. Pure Appl Chem. 1985;57:603–19.
34. Mecklenburg MF. The structure of paintings and the mechanical properties of cultural materials. Course notes from post graduate course, 21–25 November 2011, Royal Danish Academy, School of Conservation, Copenhagen.
35. Michalski S. Crack mechanism in gilding. In: Bigelow D, Come E, Landrey GJ, van Horne C, editors. Gilded wood: conservation and history. Madison: Sound View Press; 1991. p. 171–81.
36. Mecklenburg MF. Some mechanical and physical properties of gilding gesso. In: Bigelow D, Come E, Landrey GJ, van Horne C, editors. Gilded wood: conservation and history. Madison: Sound View Press; 1991. p. 163–70.
37. Mecklenburg MF, Tumosa CS, Vicenzi EP. The influence of pigments and ion migration on the durability of drying oil and alkyd paints. In: Mecklenburg MF, Charola AE, Koestler RJ, editors. New insights into the cleaning of paintings, proceedings from the cleaning 2010 international conference, Universidad Politécnica de Valencia and Museum Conservation Institute. Washington, DC: Smithsonian Institution Scholarly Press; 2013. p. 59–67.
38. Krzemień L, Łukomski M, Bratasz Ł, Kozłowski R, Mecklenburg MF. Mechanism of craquelure pattern formation on panel paintings. Stud Conserv. 2016;61(6):324–30.

Publisher's Note